

Highly Specific Plasmonic Biosensors for Ultrasensitive microRNA Detection in Plasma from Pancreatic Cancer Patients

Supporting Information

Gayatri K. Joshi¹, Samantha Deitz-McElyea², Merrell Johnson,³ Sonali Mali¹, Murray Korc^{2,*}, and Rajesh Sardar^{1,4,*}

¹Department of Chemistry and Chemical Biology, Indiana University-Purdue University Indianapolis, 402 N. Blackford Street, LD 326, Indianapolis, IN 46202

²Indiana University School of Medicine, 980 W. Walnut Street, C549, Indianapolis, IN 46202

³Department of Physics, Indiana University-Purdue University Indianapolis, 402 N. Blackford Street, LD 326, Indianapolis, IN 46202

⁴Integrated Nanosystems Development Institute, Indiana University-Purdue University Indianapolis, 402 N. Blackford Street, Indianapolis, Indiana 46202, United States

Corresponding author email: mkorc@iu.edu (M.K.); rsardar@iupui.edu (R.S.)

Table of Contents

S1. Chemicals.

S2. Nucleic Acid Sequences

S3. Spectroscopy and Microscopy Characterization

S4. Synthesis of Gold Nanoprisms

S5. Silanization of Glass Coverslips and Attachment of Nanoprisms

S6. Preparation of microRNA Sensors

S7. Detection of Synthetic microRNAs in Either PBS (pH = 7.4) buffer, 40% Bovine Plasma, and 40% Human Plasma

S8. Confirming DNA:RNA Duplex and Regeneration of the Sensors

S9. microRNA Detection of Total RNAs Extracted and Purified Pancreatic Cancer Patients in PBS Buffer

S10. microRNA Detection in Human plasma collected from Pancreatic Cancer Patients without RNAs Extraction

S11. Data processing and statistical analysis.

S12. Experimental Data to Develop Calibration Curves

S1. Chemicals. Chloro(triethylphosphine) gold (I) (Et_3PAuCl , 97%), poly(methylhydrosiloxane) (PMHS, Mn = 1700-3300), trioctylamine (TOA, 98%), ACS grade acetonitrile (CH_3CN , 99.9%), methanol (99.8%), human plasma (contains 4% trisodium citrate and tested for HIV, hepatitis C and hepatitis B), thiol modified ssDNAs, microRNAs (miRs), Tris-base, magnesium chloride (MgCl_2), potassium chloride (KCl), ethylenediaminetetraacetic acid (EDTA), and bovine plasma (contain 3.8% trisodium citrate as an anticoagulant) were purchased from Sigma Aldrich and were used as received. (3-mercaptopropyl)-triethoxysilane (MPTES, 94%) was purchased from Alfa Aesar, and ethanol (alcohol 200 proof) was purchased from Decon labs. RNase H enzyme and RNase H reaction buffer were purchased from New England bio labs inc. RNase free sterile water was obtained from Baxter Healthcare Corporation. 1, 4-Dithiothreitol (DTT) was purchased from Roche Diagnostics. Hydrochloric acid (HCl), sodium chloride (NaCl , $\geq 99.5\%$), sodium phosphate monobasic monohydrate ($\text{NaH}_2\text{PO}_4 \cdot \text{H}_2\text{O}$, $>98\%$), sodium phosphate dibasic anhydrous (Na_2HPO_4), and the glass coverslips were purchased from Fisher Scientific. RBS 35 Detergent was obtained from Thermo Scientific and used as received. The super Sharpe silicon scanning probes (SSS-NCHR) for atomic force microscopy measurements were purchased from nanosensors. All water was purified using a Thermo Scientific Barnstead Nanopure system. Thiol modified oligonucleotides and all miRs were stored at -20°C . RNase free sterile water was used to prepare the PBS buffer solution. Polyethylene glycol thiol ($\text{PEG}_6\text{-SH}$) was synthesized in our laboratory using published procedures.¹

S2. Nucleic Acid Sequences

Table S1. Summary of oligonucleotide and miR strands used in this study

strand	name	sequence	MW (kDa)	modification
A	ssDNA-21	5'-TCAACATCAGTCTGATAAGCTA-3'	6.7	5'thiol- C_6
B	ssDNA-10b	5'-CACAAATTCGGTTCTACAGGGTA-3'	7.1	5'thiol- C_6
C	target miR-21	5'-UAGCUUAUCAGACUGAUGUUGA-3'	6.6	none
D	target miR-10b	5'-UACCCUGUAGAACCGAAUUUGUG-3'	7.0	none
E	miR-16	5'-UAGCAGCACGUAAAUAUUGGCG-3'	7.1	none
F	miR-126	5'-CAUUAUUACUUUUGGUACGCG-3'	6.3	none
G	miR-141	5'-UAACACUGUCUGGUAAAGAUGG-3'	6.7	none
H	miR-122	5'-UGGAGUGUGACAAUGGUGUUUG-3'	6.8	none

S3. Spectroscopy and Microscopy Characterization. Absorption and extinction spectra in the range of 300-1100 nm were collected with a Varian Cary 50 Scan UV-visible spectrophotometer using 1 cm quartz cuvette. All the absorbance spectra were collected

using 0.3 mL of reaction solution diluted in 2.0 mL of acetonitrile. Acetonitrile was used as a background for these measurements, and the background was run before collecting the absorbance spectra. All extinction spectra were measured in PBS buffer (pH 7.2) at room temperature unless otherwise specified. Here, the blank silanized glass coverslips immersed in PBS buffer were used as a background and the background was run before collecting the extinction spectra. The chemically synthesized gold nanoprisms attached onto the silanized glass coverslips were characterized after each functionalization step through atomic force microscopy (AFM). All AFM measurements were conducted in air utilizing tapping mode on a Bruker BioScope Catalyst with SSS-NCHR probes (Nanosensors) (tip radius ~ 2 nm). Images were collected using a tip velocity of 1 mM/s over 1-2 μM scan sizes of three to five regions of each samples. All microscopy files were plain fitted and 2D fitted using Gwyddion. Also using the software, the individual nanoprisms were selected and analyzed to determine their surface area and height profiles.

S4. Synthesis of Gold Nanoprisms. Gold nanoprisms were chemically synthesized according to our previously developed procedure with minor modification.²⁻³ Specifically, $\text{Et}_3\text{PAu(I)Cl}$ (8 mg, 0.02 mmol) was dissolved in 5 mL of acetonitrile and allowed to stir for 5 min at room temperature. 0.085 mL of TOA and 0.3 mL of PMHS were mixed with 1 mL of acetonitrile in a vial and injected into the above solution. The reaction mixture was then allowed to heat at 40 °C. The solution color started to change from colorless to pink, purple, blue and at this point 14 mL acetonitrile was added to the reaction and the reaction was allowed to run for another 130 min, which resulted in a dark blue solution indicating the formation of nanoprisms with a stable absorbance dipole peak at 780 nm in acetonitrile (Figure S1). The solution was then removed from heat, centrifuged at 7000 rpm for 2 minutes, and used for the biosensor fabrication.

S5. Silanization of Glass Coverslips and Attachment of Nanoprisms. The glass coverslips (supporting substrates) were functionalized according to our previously published procedures.²⁻⁵ Glass coverslips were immersed in a 20% (v/v) aqueous RBS 35 detergent solution at 90 °C for 30 min, followed by 5 min of sonication. After thoroughly rinsing the coverslips with nanopure water, they were placed in a solution of conc. hydrochloric acid and methanol (1:1 v/v) for 30 min. The coverslips were then rinsed several times with nanopure water and dried in a vacuum oven at 60 °C overnight then incubated in a solution of 10% MPTES in ethanol for 30 min, sonicated for 5 min, and rinsed with anhydrous ethanol. The coverslips were rinsed with ethanol by sonicating them in ethanol, which was repeated at least 5 times. After rinsing, the coverslips were baked in a vacuum oven at 120 °C for 3 hours. The MPTES-functionalized coverslips (substrate) were then incubated for 30 min in a freshly prepared gold nanoprisms reaction solution. After incubation, the substrate-bound gold nanoprisms were rinsed with ethanol, dried under nitrogen flow, and stored under nitrogen at 4 °C.

S6. Preparation of microRNA Sensors. As the reaction solution contains other non-prismatic nanostructures, a tape-cleaning procedure was performed on the substrate bound gold nanoprisms platform to remove non-prismatic nanostructures. Tape cleaning was done by placing the adhesive (scotch) tape onto the gold nanoprisms attached supporting substrate, gently pressed down with a finger, and slowly removed at a 90°

angle.⁴ The nanoprisms containing supporting substrates were then incubated into PBS buffer solution containing HS-C6-ssDNA-X: PEG₆-SH (1 μ M each) for overnight. Next, the HS-C6-ssDNA-X: PEG₆-SH functionalized gold nanoprisms (plasmonic biosensor for miR-X) were rinsed with copious amount of PBS buffer to remove loosely bound reactants and biosensors then further utilized for miR-X sensing.

S7. Detection of Synthetic microRNAs in Either PBS (pH = 7.4) buffer, 40% Bovine Plasma, and 40% Human Plasma. Different concentrations of synthetic miR-X solutions were prepared either in PBS buffer, or 40 % bovine plasma, or 40 % human plasma. The plasmonic biosensors prepared in S6 were then incubated in the different concentrations of miR-X solutions in above-mentioned physiological media overnight. The miR-X bound biosensors were then rinsed with PBS buffer to remove any non-specifically adsorbed species and placed in PBS buffer for 10 min to equilibrate. Extinction spectra were collected in PBS buffer.

S8. Confirming DNA-RNA Duplex and Regeneration of the Sensors. In order to confirm the miR-X hybridization with the plasmonic biosensor, hybridized, dehybridized, and rehybridized with target miR-X were investigated. RNase H enzyme that selectively cleaves the DNA: RNA duplex was used for dehybridization studies. The plasmonic biosensor for miR-21 was allowed to hybridize in 100 nM of miR-21 in 40% human plasma overnight. The plasmonic biosensor's response (λ_{LSPR}) was measured before and after the incubation in miR-21. To confirm that the λ_{LSPR} shift observed after miR-21 incubation was indeed due to its hybridization with the gold nanoprisms' surface bound HS-C₆-ssDNA-21 probe, the miR-21 bound plasmonic biosensor was immersed in 15 units of RNase H suspended 20mM of Tris-HCl (pH 7.4), 20mM KCl, 10mM MgCl₂, 0.1mM EDTA, and 0.1 mM DTT solution for 2h, then rinsed with PBS buffer and the λ_{LSPR} shift was measured. The plasmonic biosensor was further incubated in 100 nM miR-21 solutions of 40% human plasma overnight. The same process was repeated for several cycles to confirm the stability and the regeneration of the plasmonic biosensor. Control experiments without hybridized miR-21 were also performed, where the plasmonic biosensor for miR-21 was immersed in RNase H containing reaction solution for overnight followed by rinsing with PBS buffer. The biosensor was further immersed in 100 nM miR-21 solutions in 40% human plasma overnight, rinsed with PBS buffer and the $\Delta\lambda_{\text{LSPR}}$ shift was measured.

S9. microRNA Detection of Total RNAs Extracted and Purified Pancreatic Cancer Patients plasma in PBS Buffer. The plasma samples were collected from six PDAC patients and six normal control subjects. Total plasma RNAs including miRs were extracted from 100 μ L of each plasma sample using TRIZOL kit, with a final elution volume of 28 μ L. 14 μ L volumes were used for the miR quantification using the plasmonic biosensor and the remaining 14 μ L were used for qRT-PCR assay to confirm the miR levels in each sample. 14 μ L volumes were diluted in 786 μ L of PBS buffer and the prepared plasmonic biosensor for miR-X was incubated in that solution overnight, followed by rinsing with PBS buffer and λ_{LSPR} measurements in PBS buffer.

S10. microRNA Detection in Human plasma collected from Pancreatic Cancer

Patients without RNAs Extraction. 50 μL of human plasma samples were obtained from the six PDAC patients. 50 μL of aliquot was diluted with 750 μL of PBS buffer and the plasmonic biosensor prepared for miR-21 was immobilized in these solutions overnight and then rinsed with PBS buffer. λ_{LSPR} responses of the biosensor for each plasma sample were measured in PBS buffer. The experiment was repeated at least four times and the obtained λ_{LSPR} responses were further correlated with the results obtained for same samples through qRT-PCR assay.

S11. Data processing and statistical analysis. All measurements for synthetic miRs were repeated at least five times, and the PDAC patients' samples were measured at least four times. The obtained responses were reported as mean \pm S.D. for each step. The λ_{LSPR} peak position was determined by taking the maxima of the dipole peak position in the UV-visible spectra. The $\Delta\lambda_{\text{LSPR}}$ was derived by taking the difference between the plasmonic biosensors response towards the λ_{LSPR} before and after hybridization with the standard target miR-X to the functionalized surface ssDNA-X probe. All UV-visible spectra and the calibration curves were plotted using the MS-Excel. The extinction spectra were adjusted to the highest extinction value to visualize the λ_{LSPR} shift. The LOD was calculated by measuring the $\Delta\lambda_{\text{LSPR}}$ for the blank and then obtained the Z (mean + 3σ) value and convert the Z value into the relative concentration using the calibration curve. Here, the blank measurement was the λ_{LSPR} response for HS-C6-ssDNA-X: PEG₆-SH functionalized gold nanoprisms before and after overnight incubation in the relative physical media without target miR-X. The relative concentration for miR-X for total RNAs extracted from PDAC patient plasma and normal control subject plasma samples were derived from the calibration curve obtained for synthetic miR-X in PBS buffer. However, the calibration curve for synthetic miR-21 in 40% human plasma was used to derive the relative concentrations for miR-21 in PDAC patients' plasma without any extraction.

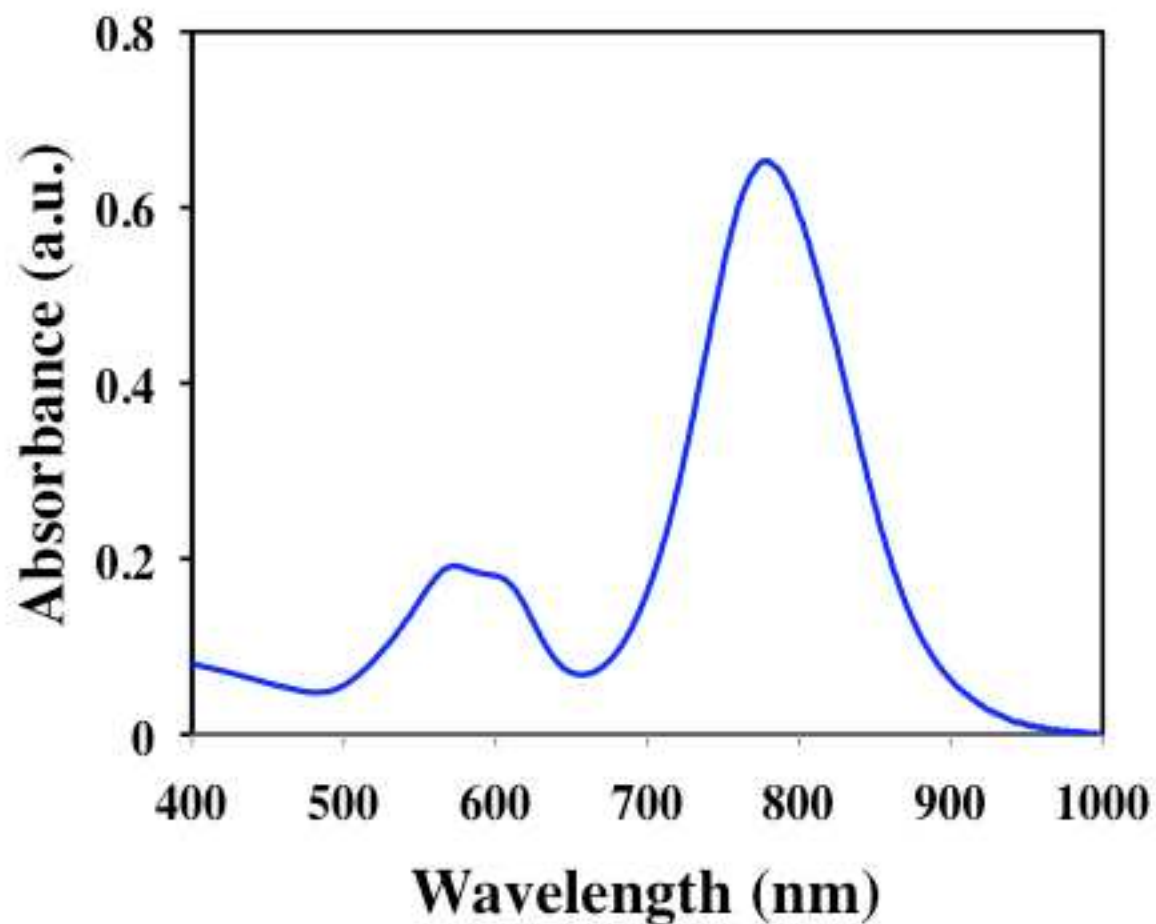
Supporting Information Figures

Figure S1: UV-visible absorption spectrum of chemically synthesized gold nanoprisms in acetonitrile. The gold nanoprisms displayed the dipole λ_{LSPR} peak at 780 nm.

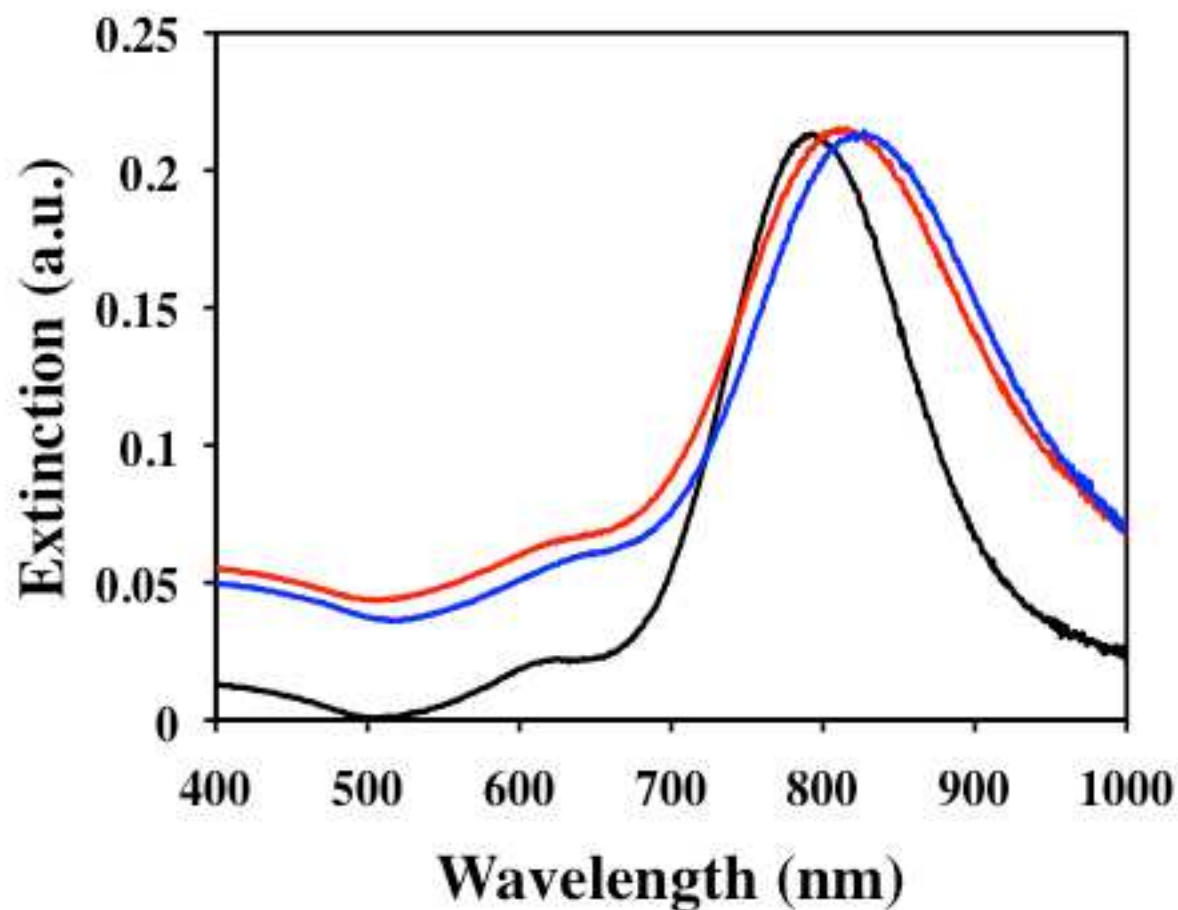


Figure S2: UV-visible extinction spectra of gold nanoprisms attached onto silanized glass substrate (black, $\lambda_{\text{LSPR}} = 799$ nm), functionalized with 1:1 μM of HS-C6-ssDNA-10b: PEG₆-SH (red, $\lambda_{\text{LSPR}} = 821$ nm), and after incubation into 100 nM miR-10b solution in PBS buffer (blue, $\lambda_{\text{LSPR}} = 836$ nm). All extinction spectra were measured in PBS buffer.

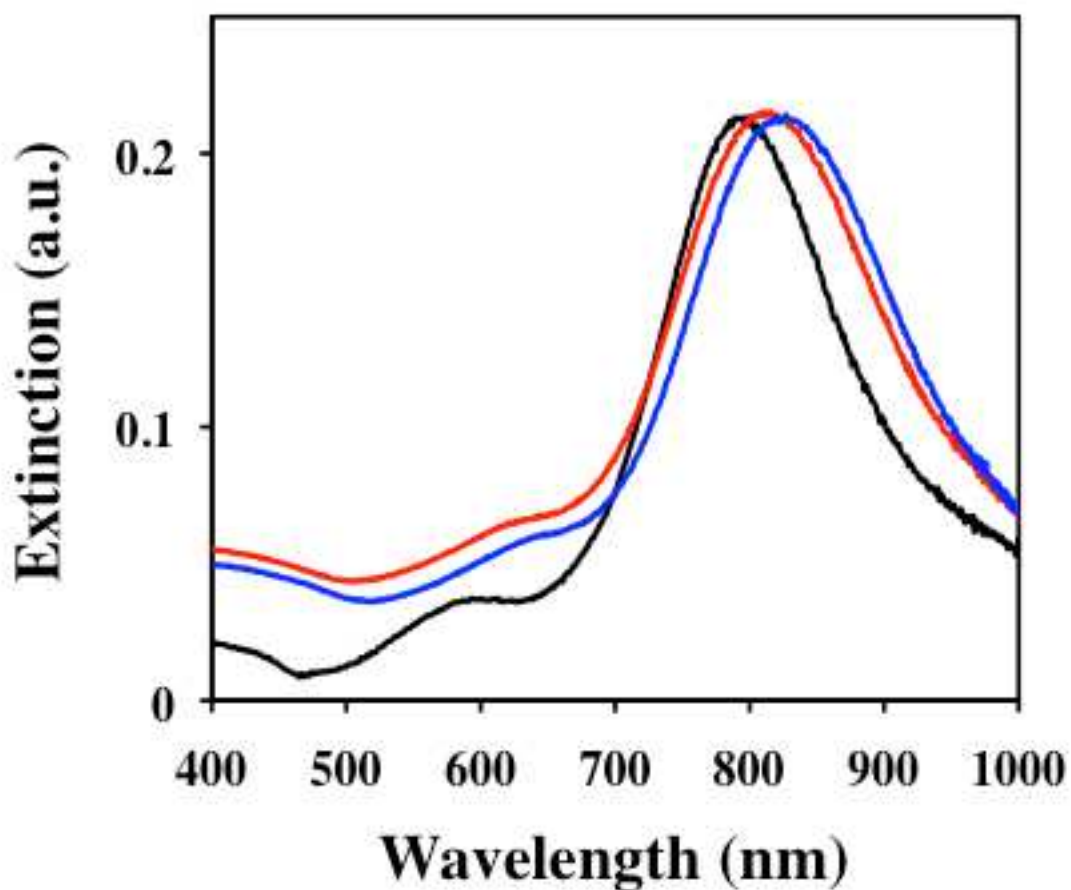


Figure S3: UV-visible extinction spectra of gold nanoprisms attached on silanized glass substrate (black, $\lambda_{\text{LSPR}} = 802$ nm), functionalized with 1:1 μM of HS-C6-ssDNA-21: PEG₆-SH (red, $\lambda_{\text{LSPR}} = 823$ nm), and after incubation into 100 nM miR-21 solution in 40% human plasma (blue, $\lambda_{\text{LSPR}} = 836$ nm). All extinction spectra were measured in PBS buffer.

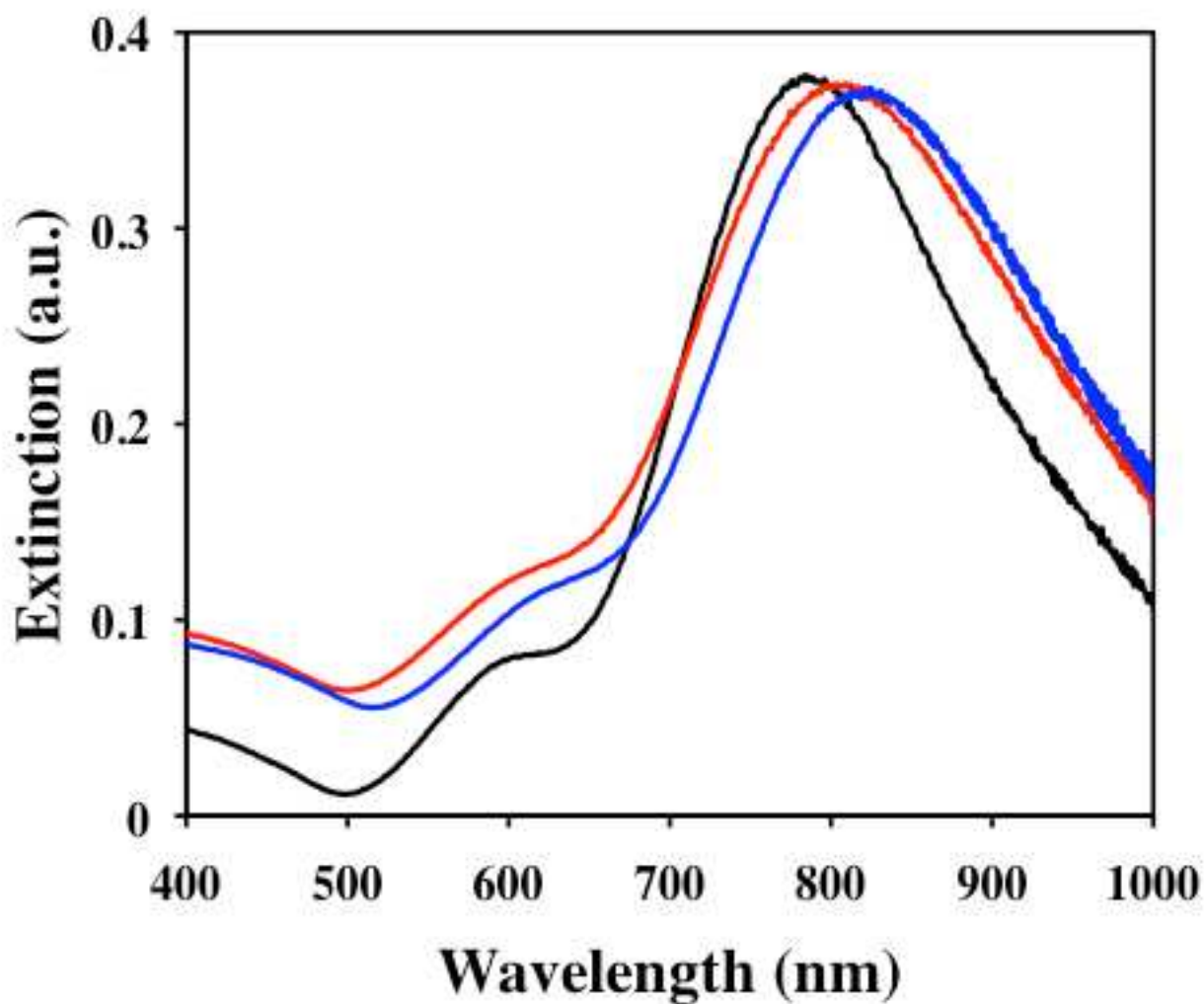


Figure S4: UV-visible extinction spectra of gold nanoprisms attached onto silanized glass substrate (black, $\lambda_{\text{LSPR}} = 802$ nm), functionalized with 1:1 μM of HS-C6-ssDNA-10b: PEG₆-SH (red, $\lambda_{\text{LSPR}} = 817$ nm), and after incubation into 100 nM miR-10b solution in 40% human plasma (blue, $\lambda_{\text{LSPR}} = 829$ nm). All extinction spectra were measured in PBS buffer.

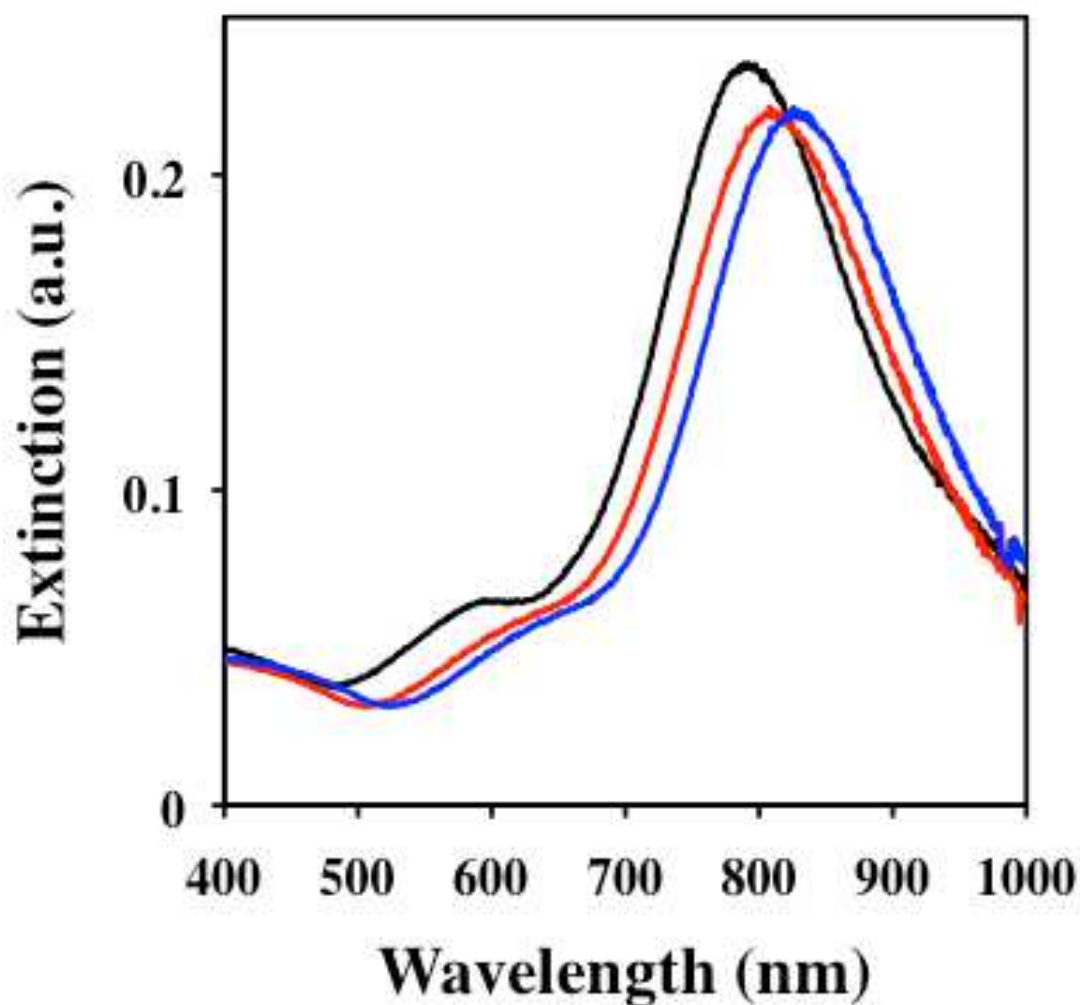


Figure S5: UV-visible extinction spectra of gold nanoprisms attached onto silanized glass substrate (black, $\lambda_{\text{LSPR}} = 800$ nm), functionalized with 1:1 μM of HS-C6-ssDNA-21: PEG₆-SH (red, $\lambda_{\text{LSPR}} = 819$ nm), and after incubation into 100 nM miR-21 solution in 40% bovine plasma (blue, $\lambda_{\text{LSPR}} = 835$ nm). All extinction spectra were measured in PBS buffer.

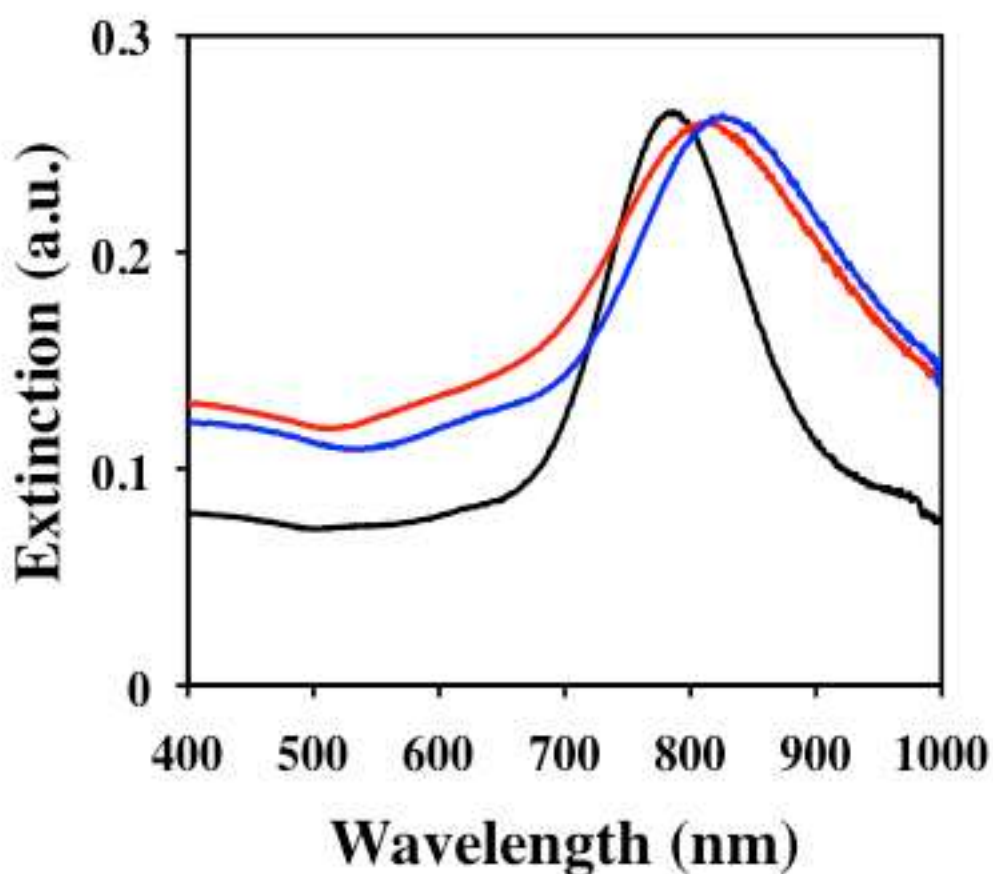


Figure S6: UV-visible extinction spectra of gold nanoprisms attached onto silanized glass substrate (black, $\lambda_{\text{LSPR}} = 798$ nm), functionalized with 1:1 μM of HS-C6-ssDNA-10b: PEG₆-SH (red, $\lambda_{\text{LSPR}} = 820$ nm), and after incubation into 100 nM miR-10b solution in 40% bovine plasma (blue, $\lambda_{\text{LSPR}} = 832$ nm). All extinction spectra were measured in PBS buffer.

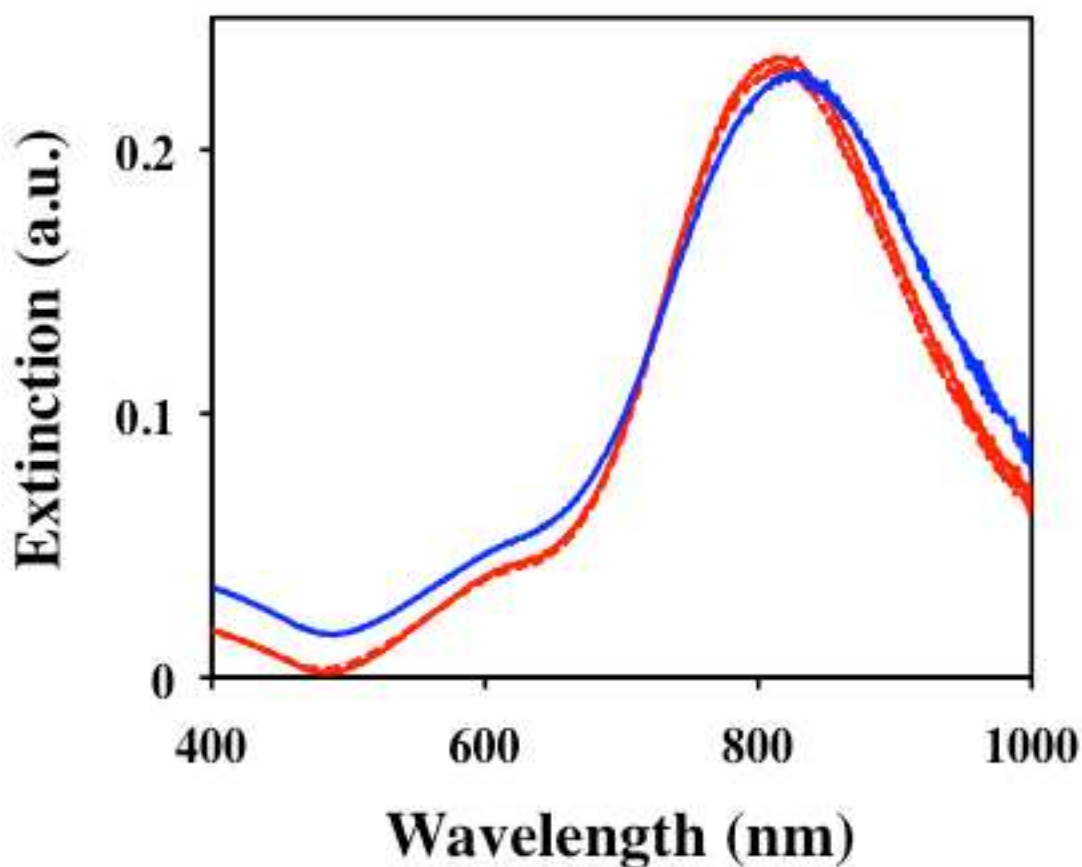


Figure S7: UV-visible extinction spectra of gold nanoprisms attached on silanized glass substrate functionalized with 1:1 ratio of HS-C6-ssDNA-21: PEG₆SH (red, $\lambda_{\text{LSPR}} = 818$ nm), after incubation in 15 units of RNase H solution overnight (red dotted, $\lambda_{\text{LSPR}} = 818$ nm), and after incubation in 100 nM of miR-21 in 40% human plasma solution (blue, $\lambda_{\text{LSPR}} = 832$ nm).

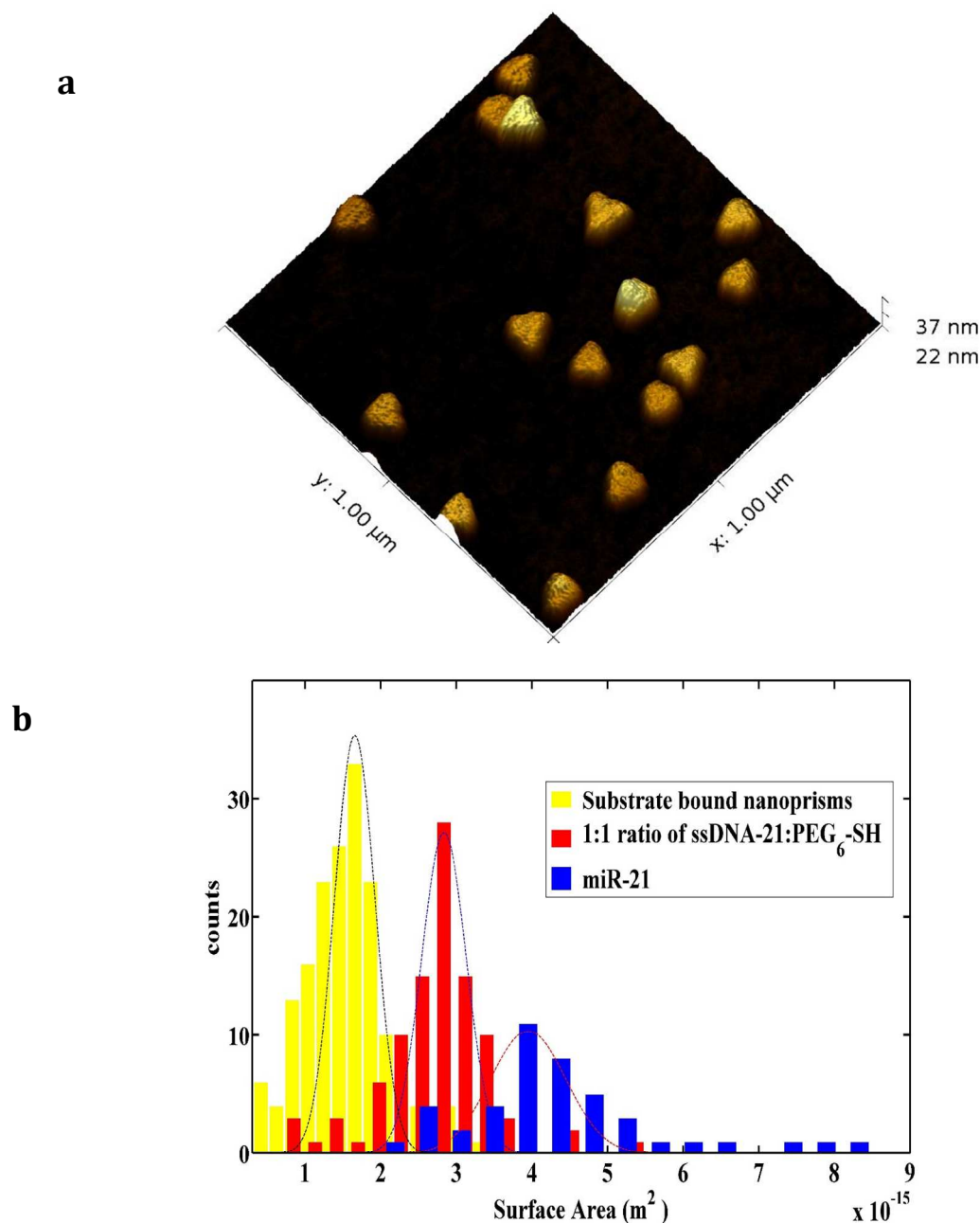


Figure S8: (a) Atomic force microscopy image of gold nanoprisms attached onto silanized glass substrate without any surface modification. **(b)** Histogram showing the average surface area during various functionalization steps. Forty nanoprisms were analyzed to determine the average values.

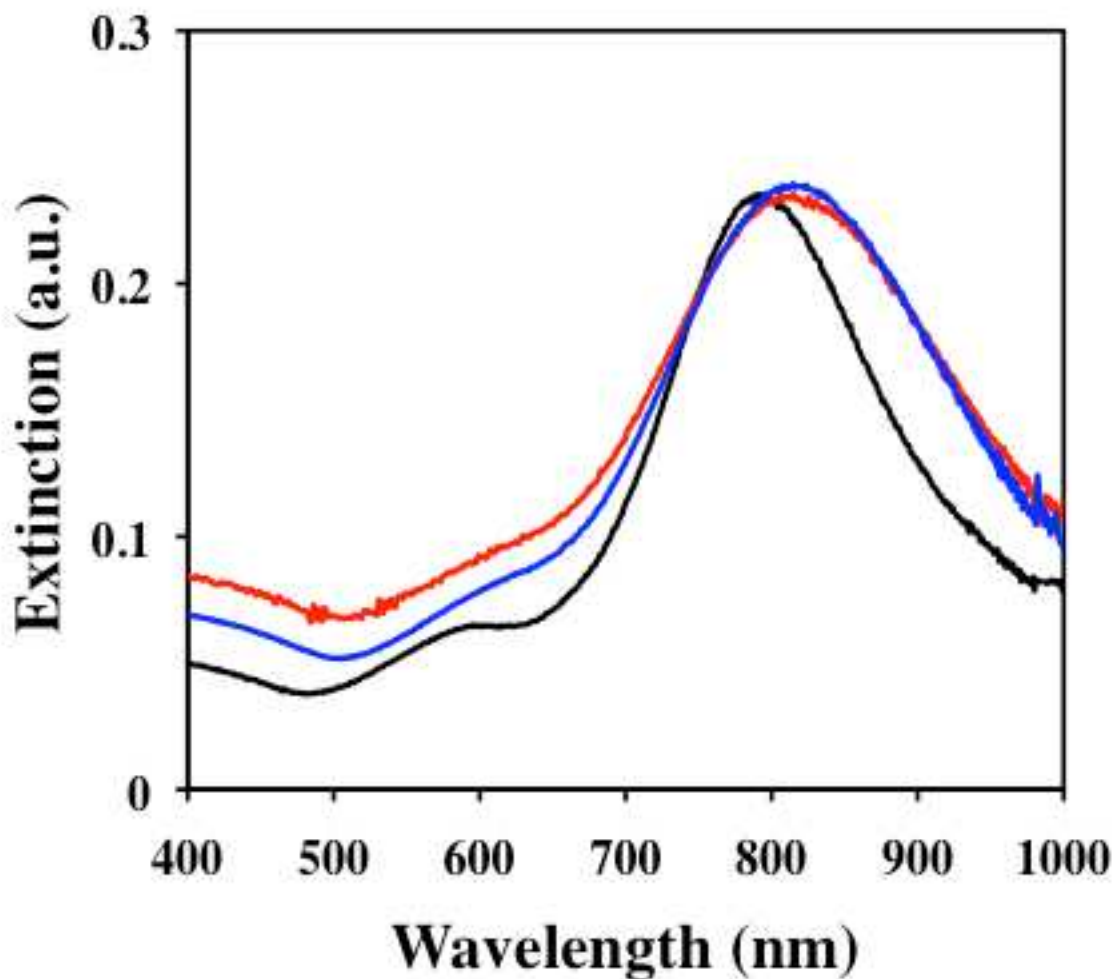


Figure S9: UV-visible extinction spectra of gold nanoprisms attached onto silanized glass substrate (black, $\lambda_{\text{LSPR}} = 800$ nm), after functionalized with 1:1 ratio of HS-C6-ssDNA-21: PEG₆ SH (red, $\lambda_{\text{LSPR}} = 822$ nm), and after incubation in 100 nM of mixed miRs (miR-16, miR-122, miR-126, miR-141) in 40% human plasma (blue, $\lambda_{\text{LSPR}} = 825$ nm).

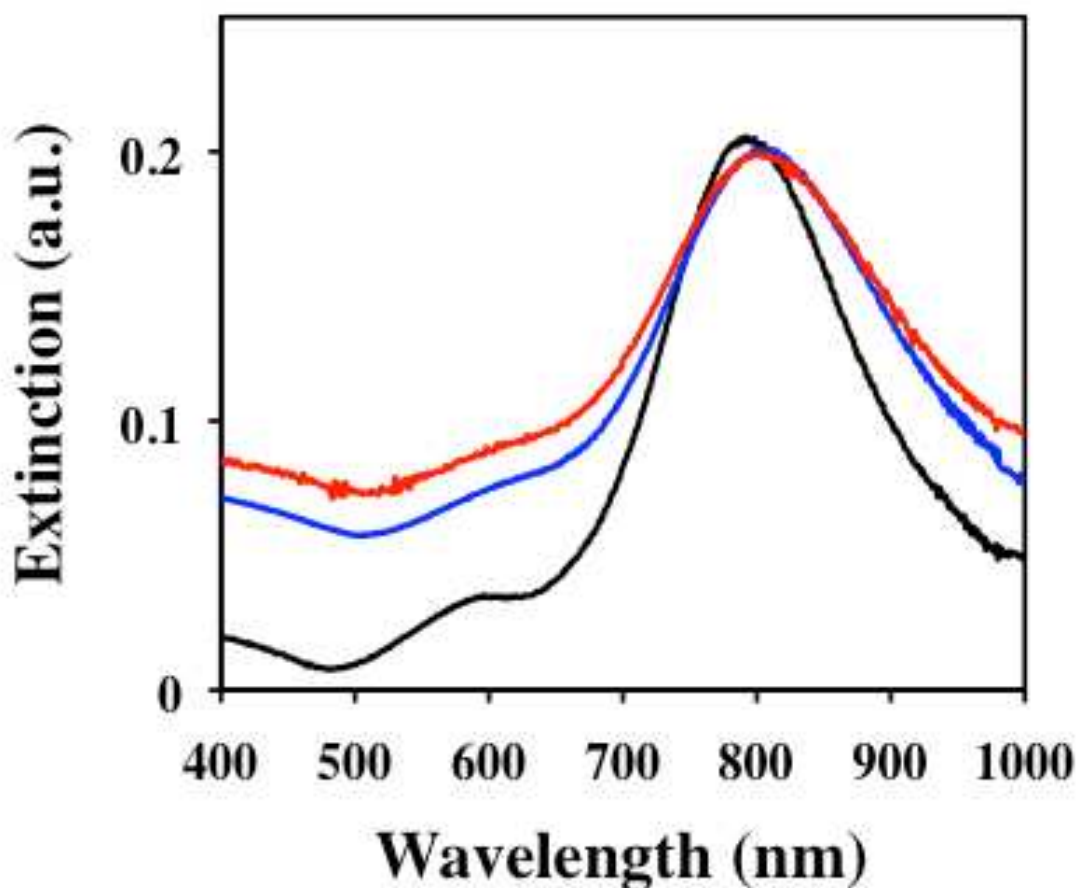


Figure S10: UV-visible extinction spectra of gold nanoprisms attached onto silanized glass substrate (black, $\lambda_{\text{LSPR}} = 799$ nm), after functionalized with $1 \mu\text{M}$ of PEG₆-SH (red, $\lambda_{\text{LSPR}} = 815$ nm), and after incubation in 100 nM of miR-21 in 40% human plasma (blue, $\lambda_{\text{LSPR}} = 816$ nm).

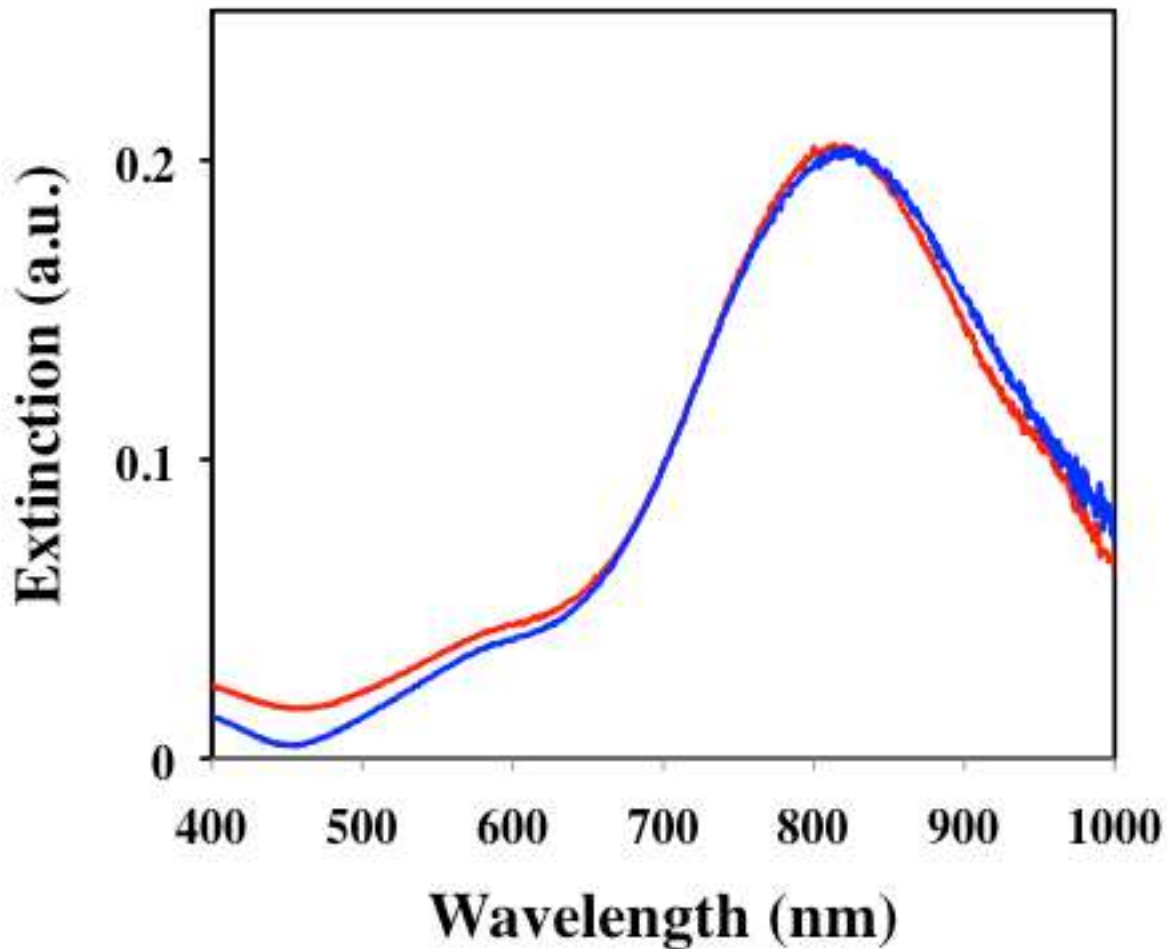


Figure S11: UV-visible extinction spectra of gold nanoprisms functionalized with 1:1 ratio of HS-C6-ssDNA-21: PEG₆-SH (red, $\lambda_{\text{LSPR}} = 820$ nm), and after incubation in extracted RNAs from human plasma collected from PDAC patient (blue, $\lambda_{\text{LSPR}} = 826$ nm).

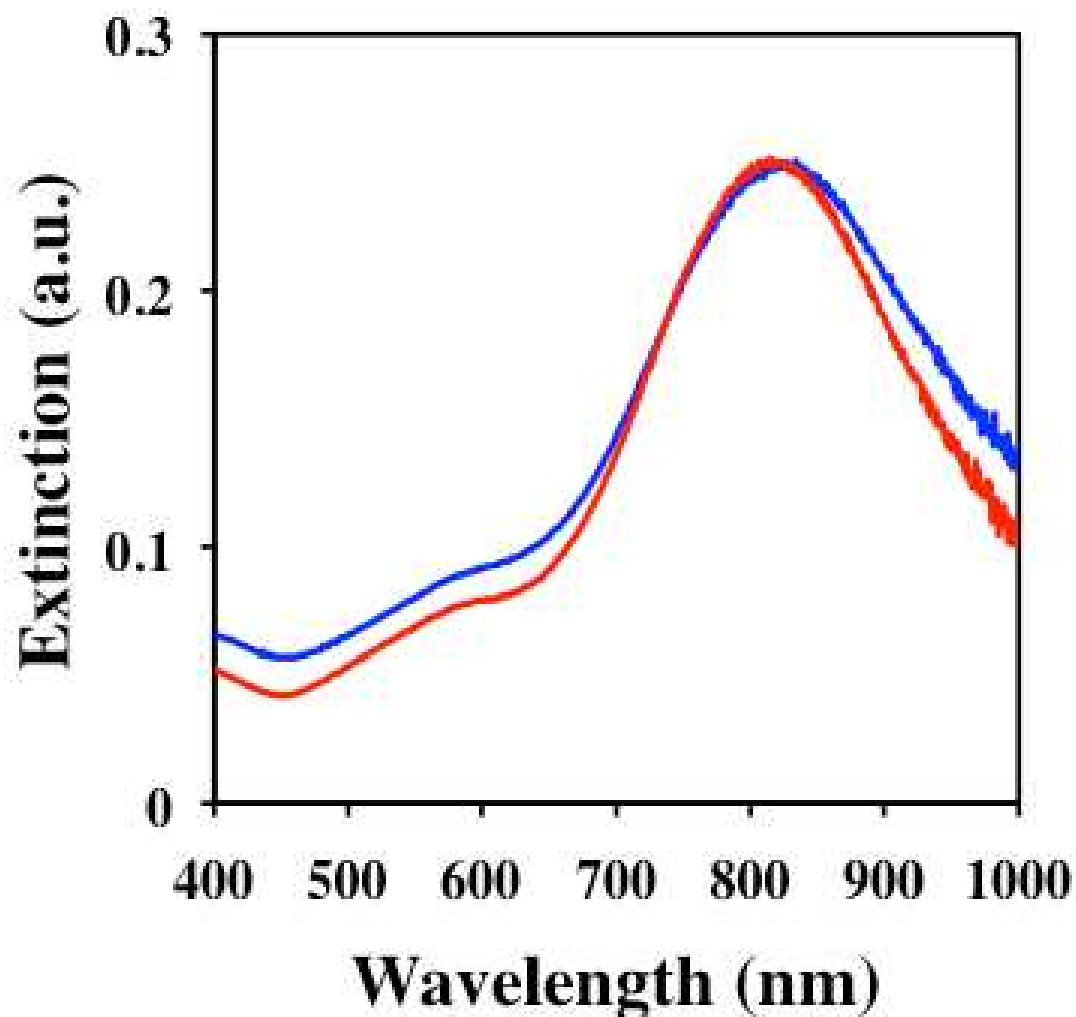


Figure S12: UV-visible extinction spectra of gold nanoprisms functionalized with 1:1 ratio of HS-C6-ssDNA-10b: PEG₆-SH (red, $\lambda_{\text{LSPR}} = 822$ nm), and after incubation in extracted RNAs from human plasma collected from PDAC patient (blue, $\lambda_{\text{LSPR}} = 829$ nm).

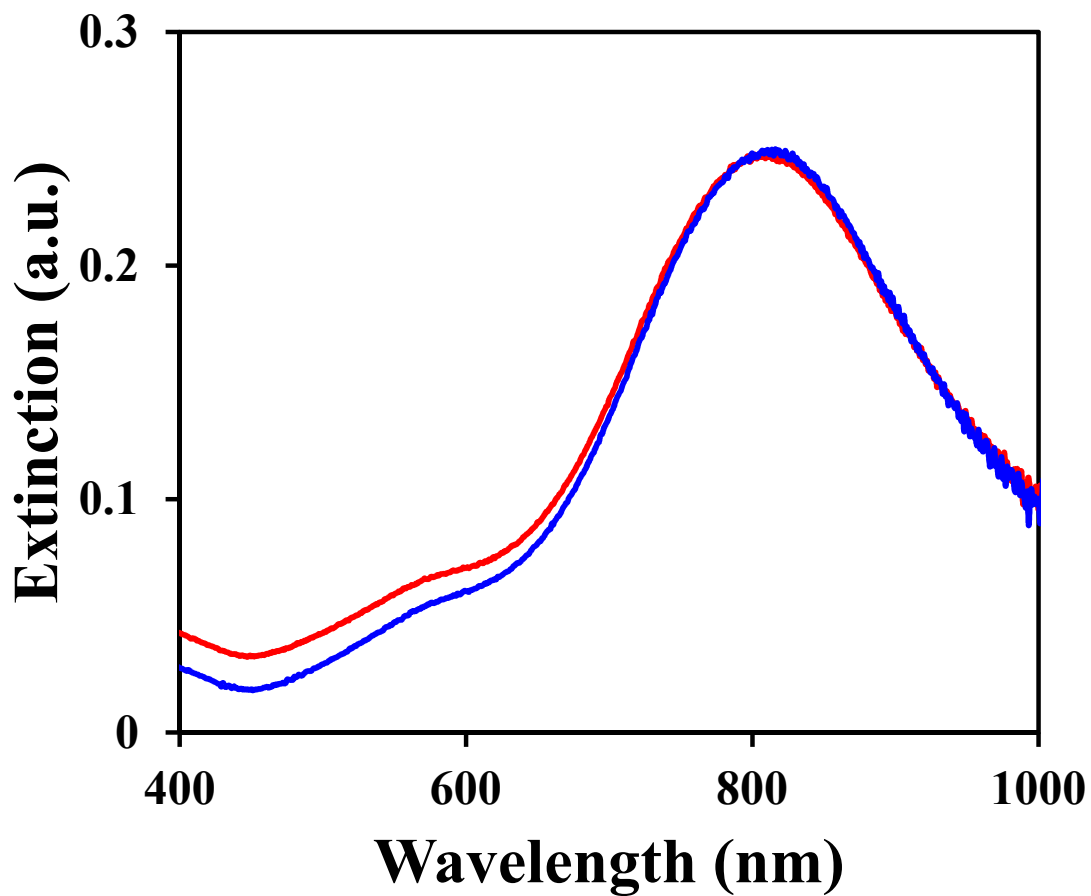


Figure S13: UV-visible extinction spectra of gold nanoprisms functionalized with 1:1 ratio of HS-C6-ssDNA-21: PEG₆-SH (red, $\lambda_{\text{LSPR}} = 816$ nm), and after incubation in human plasma sample collected from PDAC patient (blue, $\lambda_{\text{LSPR}} = 823$ nm).

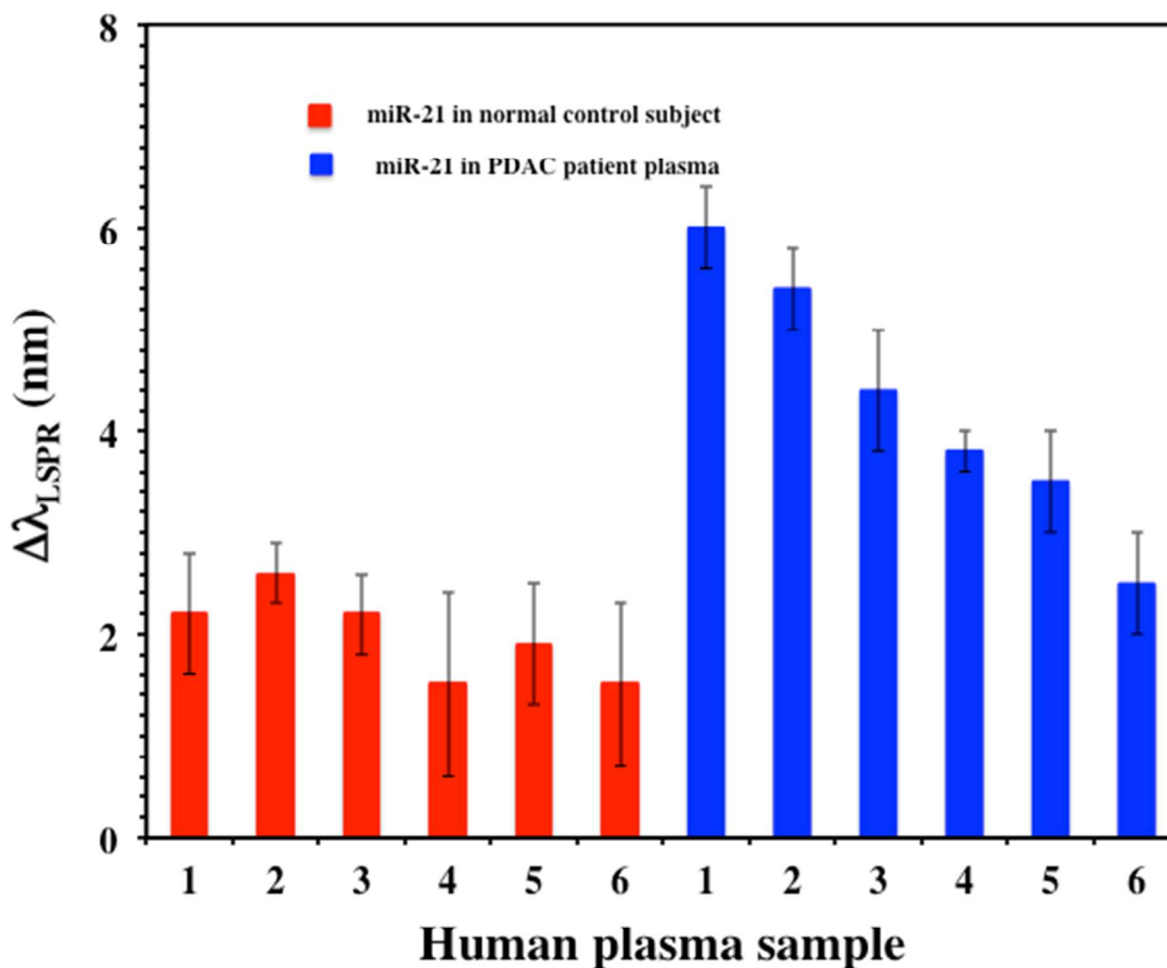


Figure S14: The average λ_{LSPR} peak shift for the miR-21 into the extracted total RNAs collected from PDAC patients (blue), and the average shift for miR-21 into the extracted RNAs collected from normal control subjects (red).

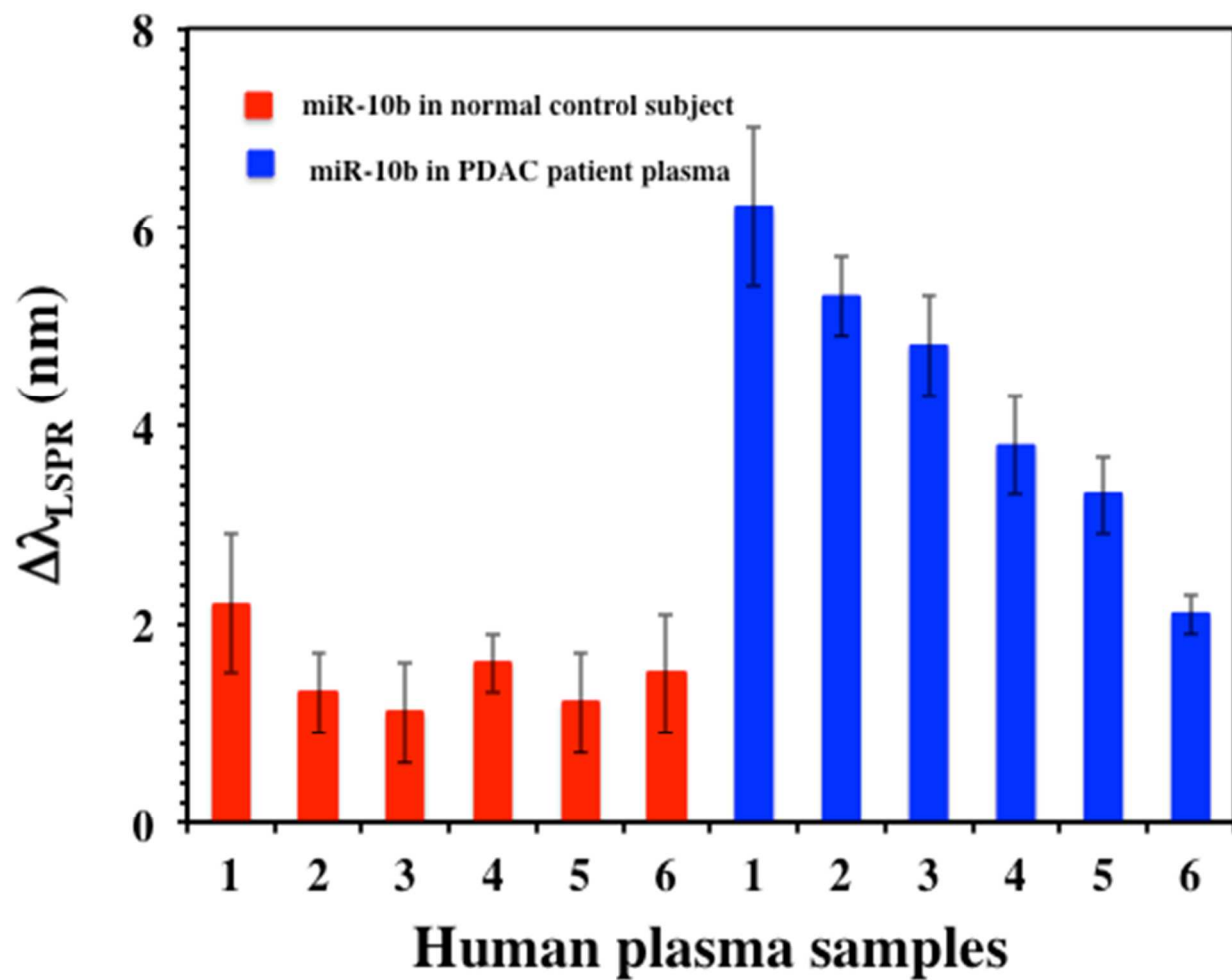


Figure S15: The average λ_{LSPR} peak shift for the miR-10b into the extracted total RNAs collected from PDAC patients (blue), and the average shift for miR-10b into the extracted RNAs collected from normal control subjects (red).

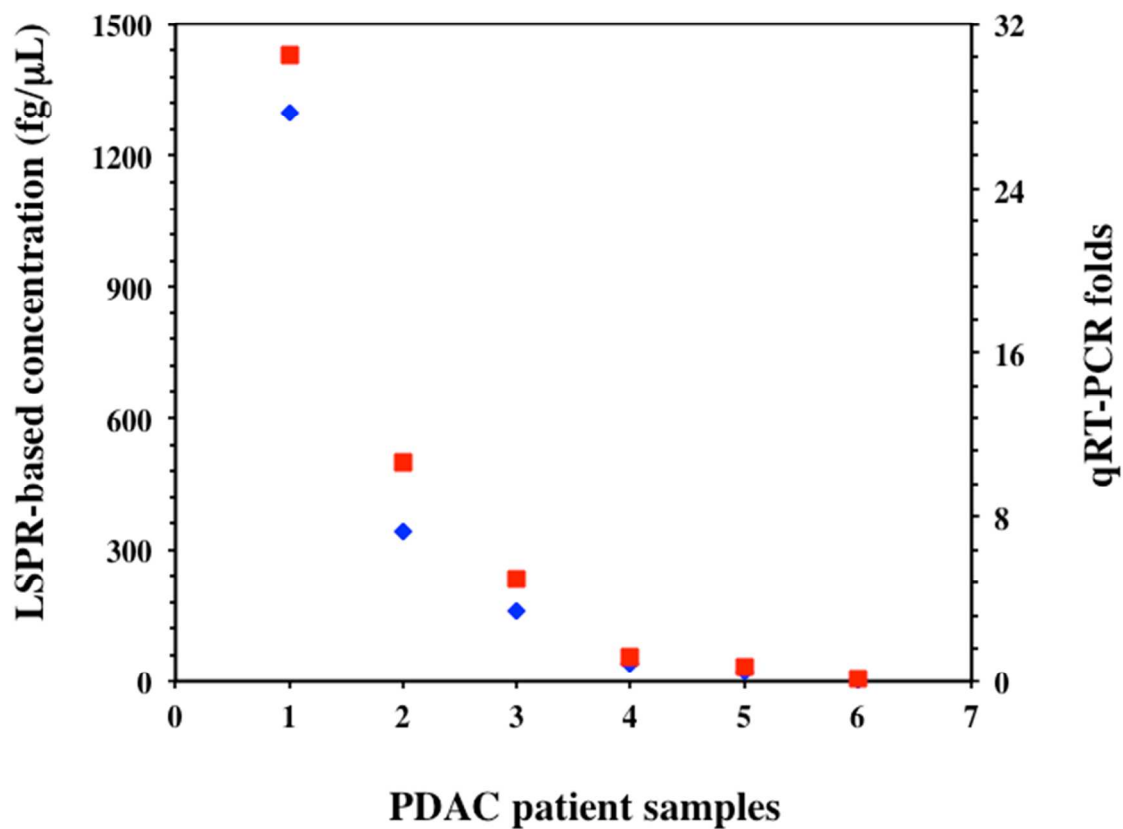


Figure S16: Comparison of miR-10b concentration for six PDAC patients determined using plasmonic biosensors (blue diamond) and qRT-PCR (red square).

Table S2. λ_{LSPR} responses from plasmonic biosensor prepared with 100% ssDNA-21 without spacer for different concentrations of miR-21 in 40% human plasma.

Sensor #	λ_{LSPR} (nm) for HS-C6-ssDNA-21 functionalized gold nanoprisms	λ_{LSPR} (nm) after incubation in different concentrations of miR-21	$\Delta\lambda_{\text{LSPR}}$ (nm)	Average $\Delta\lambda_{\text{LSPR}}$ (nm)	S.D.
		100 nM			
1	810	820	10.0		
2	811	822	11.0		
3	809	818	9.0	9.6	1.1
4	810	820	10.0		
5	809	817	8.0		
		10 nM			
1	808	817	9.0		
2	810	820	10.0		
3	808	816	8.0	7.8	1.8
4	811	817	6.0		
5	809	815	6.0		
		1 nM			
1	809	814	5.0		
2	810	814	4.0		
3	811	817	6.0	5.2	1.3
4	810	815	5.0		
5	808	814	6.0		
		0.1 nM			
1	811	816	5.0		
2	810	814	4.0		
3	810	815	5.0	4.6	0.6
4	808	812	4.0		
5	809	814	5.0		
		0.01 nM			
1	807	810	3.0		
2	808	812	4.0		
3	810	813	3.0	3.4	0.5
4	809	812	3.0		
5	808	812	4.0		

References

- (1) Lawrence, K. N.; Dolai, S.; Lin, Y.-H.; Dass, A.; Sardar, R. *RSC Adv.* **2014**, *4*, 30742-30753.
- (2) Joshi, G. K.; Blodgett, K. N.; Muhoberac, B. B.; Johnson, M. A.; Smith, K. A.; Sardar, R. *Nano Lett.* **2014**, *14*, 532-540.
- (3) Joshi, G. K.; McClory, P. J.; Dolai, S.; Sardar, R. *J. Mater. Chem.* **2012**, *22*, 923-931.
- (4) Joshi, G. K.; McClory, P. J.; Muhoberac, B. B.; Kumbhar, A.; Smith, K. A.; Sardar, R. *J. Phys. Chem. C* **2012**, *116*, 20990-21000.
- (5) Joshi, G. K.; Smith, K. A.; Johnson, M. A.; Sardar, R. *J. Phys. Chem. C* **2013**, *117*, 26228-26237.